PHILOSOPHICAL TRANSACTIONS OF THE ROYAL SOCIETY A

rsta.royalsocietypublishing.org

Research

Cite this article: Amabili M. 2013 Reduced-order models for nonlinear vibrations, based on natural modes: the case of the circular cylindrical shell. Phil Trans R Soc A 371: 20120474.
http://dx.doi.org/10.1098/rsta.2012.0474

One contribution of 17 to a Theme Issue 'A celebration of mechanics: from nano to macro'.

Subject Areas:
mechanical engineering

Keywords:
vibrations, shells, nonlinear vibrations, reduced-order models

Author for correspondence:
Marco Amabili
e-mail: marco.amabili@mcgill.ca

Reduced-order models for nonlinear vibrations, based on natural modes: the case of the circular cylindrical shell

Marco Amabili

Department of Mechanical Engineering, McGill University, 817 Sherbrooke Street West, Montreal, Quebec, Canada H3A 2K6

Reduced-order models are essential to study nonlinear vibrations of structures and structural components. The natural mode discretization is based on a two-step analysis. In the first step, the natural modes of the structure are obtained. Because this is a linear analysis, the structure can be discretized with a very large number of degrees of freedom. Then, in the second step, a small number of these natural modes are used to discretize the nonlinear vibration problem with a huge reduction in the number of degrees of freedom. This study finds a recipe to select the natural modes that must be retained to study nonlinear vibrations of an angle-ply laminated circular cylindrical shell that the author has previously studied by using admissible functions defined on the whole structure, so that an accuracy analysis is performed. The higher-order shear deformation theory developed by Amabili and Reddy is used to model the shell.

1. Introduction

Reduced-order models are essential to study nonlinear vibrations of structures and structural components. In fact, large models with many thousands or more degrees of freedom, for example obtained by commercial finite-element codes, cannot be used to calculate all the branches of the forced vibration response around a resonance of a structure. This limitation is mainly due to the huge computational problem involved and to the stiff dynamic equations obtained for large dimensional systems, because very different time scales are associated with different degrees of freedom.

A few techniques exist to build reduced-order models for nonlinear vibration problems. The most diffused ones are probably the nonlinear normal modes (under

Royal Society Publishing
Informing the science of the future

this name are classified the techniques based on the centre manifold theorem, the normal form theory and the inertial manifold) [1–9], including the most diffused version with asymptotic approach, the discretization of the equations of motion by using global (i.e. defined on the whole structure) admissible functions [10–13], the proper orthogonal decomposition method [14–18] and the natural mode discretization [19–23].

The natural mode discretization is based on a two-step analysis. In the first step, the natural modes of the structure are obtained. Because this is a linear analysis, the structure can be discretized with a very large number of degrees of freedom; for example, by using the finite-element method (FEM) or the Rayleigh–Ritz method. Then, in the second step, these natural modes, which are clearly defined on the whole structure (eventually using interpolating functions), are used to discretize the nonlinear vibration problem. The advantage is that many thousands or more degrees of freedom can be used in the linear analysis, but then just a few tens of natural modes can be retained in the nonlinear analysis with a huge reduction in the number of degrees of freedom. In fact, usually, the nonlinear vibration problems do not need many degrees of freedom to be accurately described, but the difficulty is in the choice of them. The use of natural modes, which are quite intuitive, simplifies this choice even if it does not allow the smallest dimensional problem to be obtained, as, for example, is possible by using the nonlinear normal modes. However, the advantage of having a technique that could be implemented by using natural modes obtained by commercial FEM codes is huge, and the dimension of the problem obtained by natural modes is still very small. In addition, it overcomes the limitation of the nonlinear normal modes computed with an asymptotic approach, which give inaccurate responses for large vibration amplitudes [24].

It must be clarified that, at present, there is no technique for the choice of the natural modes to be retained in the nonlinear vibration problem. This study uses the experience of the author in building reduced-order models of shell structures to find a recipe to select the natural modes that must be retained for circular cylindrical shells complete around their circumference.

The recipe works for complete circular cylindrical shells with uniform boundary conditions, isotropic or laminated, even in the presence of moderate geometrical imperfections. However, the case presented is an angle-ply laminated circular cylindrical shell that the author has previously studied by using global admissible functions [25] and here is studied by using natural modes, so that the accuracy of the solution can be studied.

Nonlinear vibrations of shells have been studied by many researchers [26–29]. Natural modes have never been used before for circular cylindrical shells, and the expansions used to discretize the shell had independent variables for each one of the displacements (and rotations). The difficulty is mostly linked to the identification of the natural modes with prevalent in-plane displacement necessary in the expansions.

The angle-ply laminated shell presents three complications. The first, which is common to closed shell structures, is that an inward vibration component with twice the excitation frequency must be retained in order to avoid unphysical excessive in-plane stretching. Here, it must be observed that shells bend much more easily than they stretch. In the case of the circular cylindrical shell, this component is axisymmetric and is associated with relatively high natural frequencies. Results will show that a few of these axisymmetric modes must be retained in the model to guarantee accurate results. The second difficulty is common to axisymmetric structures: it is the 1 : 1 internal resonance that increases the dimension of the nonlinear problem and complicates significantly the nonlinear response to external forcing. The third difficulty is linked to the angle-ply lamination, which introduces a twist in the natural mode shapes (skewed modes) that is not present for isotropic and cross-ply laminates [30]. In the present model, the refined higher-order shear deformation theory developed by Amabili & Reddy [31] is used to model the shell. A harmonic force excitation is applied at mid-length in the radial direction and simply supported boundary conditions are assumed. The equations of motion are obtained by using an energy approach based on Lagrange equations that retains dissipation. Numerical results are obtained by using the pseudo-arclength continuation method and bifurcation analysis.

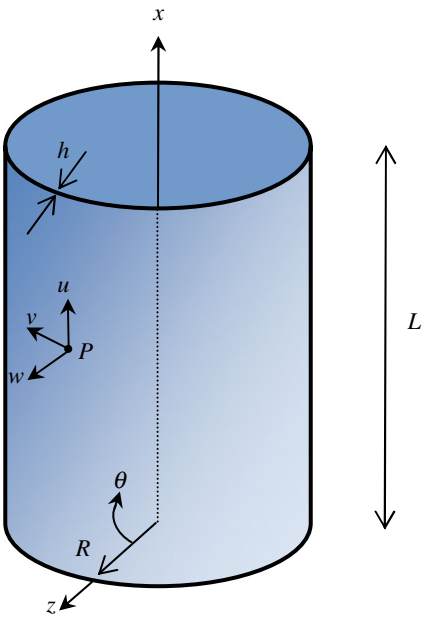

Figure 1. Circular cylindrical shell and cylindrical coordinate system. (Online version in colour.)

2. First step: natural modes

A circular cylindrical shell made of a finite number of orthotropic layers, oriented arbitrarily with respect to the shell cylindrical coordinates (x, θ, z), is considered, as shown in figure 1. Here, the theory originally developed by Amabili & Reddy [31] for shells of arbitrary shape is used; the theory is given in appendix A. The displacements of an arbitrary point P (x, θ) on the middle surface of the shell are denoted by u, v and w, in the x, θ and z directions, respectively; w is taken to be positive outward from the shell. The displacement of a generic point of the shell at distance z from the middle surface is denoted by u_x, u_θ, u_z. The kinematic relationships are presented in appendix A. Initial geometrical imperfections of the shell associated with zero initial stress are denoted by the displacement w_0 in the normal (i.e. radial) direction, also taken to be positive outward. The total thickness of the shell is indicated by h. Different techniques could be used in order to obtain the natural modes of the shell, the FEM technique being one of them. Here, the Rayleigh–Ritz method is used because the global discretization makes the mode shapes available as continuous functions expressed in closed form, which is not a necessary requirement (see [20,21,23]) but it makes the procedure easier.

Simply supported boundary conditions are assumed at the shell edges, $x = 0, L$:

$$w = 0, \tag{2.1a}$$

$$v = 0, \tag{2.1b}$$

$$\phi_2 = 0, \tag{2.1c}$$

$$N_x = 0 \tag{2.1d}$$

and

$$M_x = 0, \tag{2.1e}$$

where N_x is the axial stress resultant per unit length, and M_x is the axial stress moment resultant per unit length, that is,

$$\begin{Bmatrix} N_x \\ M_x \end{Bmatrix} = \sum_{k=1}^{K} \int_{h^{(k-1)}}^{h^{(k)}} \sigma_x^{(k)} \begin{Bmatrix} 1 \\ z \end{Bmatrix} \left(1 + \frac{z}{R}\right) \mathrm{d}z. \tag{2.2}$$

Moreover, the three displacements and the two rotations must be continuous in θ.

In order to discretize the problem by using the Rayleigh–Ritz method, the middle surface displacements and rotations u, v, w, ϕ_1 and ϕ_2 are expanded by using admissible functions, which satisfy identically only the geometrical boundary conditions in equation (2.1*a–c*). The following base of admissible shell displacements, which allows us to describe skewed modes, is used:

$$u(x,\theta,t)=\sum_{m=1}^{M}\left[u_{m,n,\mathrm{c}}\cos(n\theta)+u_{m,n,\mathrm{s}}\sin(n\theta)\right]\cos(\lambda_m x)\,\mathrm{e}^{j\omega t}, \tag{2.3a}$$

$$v(x,\theta,t)=\sum_{m=1}^{M}\left[v_{m,n,\mathrm{c}}\sin(n\theta)+v_{m,n,\mathrm{s}}\cos(n\,\theta)\right]\sin(\lambda_m x)\,\mathrm{e}^{j\omega t}, \tag{2.3b}$$

$$w(x,\theta,t)=\sum_{m=1}^{M}\left[w_{m,n,c}\cos(n\theta)+w_{m,n,s}\sin(n\theta)\right]\sin(\lambda_m x)\,\mathrm{e}^{j\omega t}, \tag{2.3c}$$

$$\phi_1(x,\theta,t)=\sum_{m=1}^{M}\left[\phi_{1_{m,n,c}}\cos(n\theta)+\phi_{1_{m,n,s}}\sin(n\theta)\right]\cos(\lambda_m x)\,\mathrm{e}^{j\omega t} \tag{2.3d}$$

and

$$\phi_2(x,\theta,t)=\sum_{m=1}^{M}\left[\phi_{2_{m,n,c}}\sin(n\theta)+\phi_{2_{m,n,s}}\cos(n\theta)\right]\sin(\lambda_m x)\,\mathrm{e}^{j\omega t}, \tag{2.3e}$$

for any number n of circumferential waves ($n=0,1,2,\ldots$), where m is the number of longitudinal half-waves ($m=1,2,\ldots$), $\lambda_m=m\pi/L$, ω is the natural frequency in rad per second, j is the imaginary unit and t is the time; $u_{m,n}$, $v_{m,n}$, $w_{m,n}$, $\phi_{1_{m,n}}$ and $\phi_{2_{m,n}}$ are the unknown coefficients that have to be determined by using the variational approach; the additional subscript 'c' or 's' indicates whether the generalized coordinate is associated with the cosine or sine function in θ except for v and ϕ_2, for which the notation is reversed. In the case of angle-ply laminated circular shells, natural modes with nodal lines inclined with respect to the x-axis (skewed modes) can appear. In order to describe them, terms with odd and even numbers of longitudinal half-waves have been inserted in equations (2.3), and a combination of sin and cos terms in the variable θ appears, but all terms will have the same circumferential wavenumber n. The presence of cosine and sine modes is the result of the symmetry of the shell and introduces, for any $n\neq 0$, couples of modes with exactly the same shape but rotated angularly by $\pi/(2n)$. These modes, being identical except for the angular position θ, have exactly the same natural frequency for a perfect shell, introducing an internal resonance of the type 1 : 1. Zero initial geometrical imperfections w_0 of the shell are considered in the radial direction in the numerical simulations.

The kinetic energy T_S of the shell, including rotary inertia, is given by

$$T_\mathrm{S}=\frac{1}{2}\sum_{k=1}^{K}\rho_\mathrm{S}^{(k)}\int_0^{2\pi}\int_0^{L}\int_{h^{(k-1)}}^{h^{(k)}}\left(\dot{u}_x^2+\dot{u}_\theta^2+\dot{u}_z^2\right)\left(1+\frac{z}{R}\right)\mathrm{d}x\,R\,\mathrm{d}\theta\,\mathrm{d}z, \tag{2.4}$$

where $\rho_\mathrm{S}^{(k)}$ is the mass density of the kth layer of the shell. The z and z^3 terms vanish after integration on z in the case of a laminate with symmetric density with respect to the z-axis. In particular, for a laminate with the same density for all the layers and uniform thickness, the following simplified expression is obtained:

$$\begin{aligned}T_\mathrm{S}=\frac{1}{2}\rho_\mathrm{S}h\int_0^{2\pi}\int_0^{L}\Bigg\{&\dot{u}^2+\dot{v}^2+\dot{w}^2+h^2\Bigg[\frac{17}{315}(\dot{\phi}_1^2+\dot{\phi}_2^2)+\left(\frac{2}{15R}\right)\dot{\phi}_1\dot{u}+\left(\frac{41}{120R}\right)\dot{\phi}_2\dot{v}\\&+\frac{1}{4}\frac{\dot{v}^2}{R^2}+\frac{\partial\dot{w}}{\partial x}\left(\frac{1}{252}\frac{\partial\dot{w}}{\partial x}-\frac{1}{30}\frac{\dot{u}}{R}-\frac{8}{315}\dot{\phi}_1\right)+\frac{1}{R}\frac{\partial\dot{w}}{\partial\theta}\left(\frac{1}{252R}\frac{\partial\dot{w}}{\partial\theta}+\frac{\dot{v}}{120R}-\frac{8}{315}\dot{\phi}_2\right)\Bigg]\Bigg\}R\,\mathrm{d}\theta\,\mathrm{d}x\\&+O(h^5).\end{aligned} \tag{2.5}$$

The stress–strain relations for the kth orthotropic lamina of the shell, in the material principal coordinates (1,2,3), are obtained under the hypothesis $\sigma_3 = 0$ [31],

$$\begin{Bmatrix} \sigma_1 \\ \sigma_2 \\ \tau_{23} \\ \tau_{13} \\ \tau_{12} \end{Bmatrix}^{(k)} = \begin{bmatrix} c_{11} & c_{12} & 0 & 0 & 0 \\ c_{21} & c_{22} & 0 & 0 & 0 \\ 0 & 0 & G_{23} & 0 & 0 \\ 0 & 0 & 0 & G_{13} & 0 \\ 0 & 0 & 0 & 0 & G_{12} \end{bmatrix}^{(k)} \begin{Bmatrix} \varepsilon_{11} \\ \varepsilon_{22} \\ \gamma_{23} \\ \gamma_{13} \\ \gamma_{12} \end{Bmatrix}, \tag{2.6}$$

and

$$c_{11} = \frac{E_1}{1 - \nu_{12}\nu_{21}}, \quad c_{12} = c_{21} = \frac{E_2\nu_{12}}{1 - \nu_{12}\nu_{21}}, \quad c_{22} = \frac{E_2}{1 - \nu_{12}\nu_{21}} \quad \text{and} \quad \nu_{ij}E_j = \nu_{ji}E_i, \tag{2.7}$$

where G_{12}, G_{13} and G_{23} are the shear moduli in the 1–2, 1–3 and 2–3 directions, respectively, and the superscript (k) refers to the kth layer within a laminate. Equation (2.6) is obtained (i) under the transverse isotropy assumption with respect to planes orthogonal to axis 1, i.e. assuming fibres in the direction parallel to axis 1, so that $E_2 = E_3$, $G_{12} = G_{13}$ and $\nu_{12} = \nu_{13}$, and (ii) by solving the constitutive equations for ε_{33} as a function of ε_{11} and ε_{22} and then eliminating it.

Equation (2.6) can be transformed to the shell coordinates (x, θ, z) by the following equation [31]:

$$\begin{Bmatrix} \sigma_x \\ \sigma_\theta \\ \tau_{\theta z} \\ \tau_{xz} \\ \tau_{x\theta} \end{Bmatrix}^{(k)} = [Q]^{(k)} \begin{Bmatrix} \varepsilon_{xx} \\ \varepsilon_{\theta\theta} \\ \gamma_{\theta z} \\ \gamma_{xz} \\ \gamma_{x\theta} \end{Bmatrix}, \tag{2.8}$$

where the strain components in the shell coordinates are related to the shell generalized displacement in appendix A by using the Amabili–Reddy nonlinear shell theory; in particular, here all the nonlinear terms in the strain–displacement relationships in appendix A are neglected in the calculation of the natural modes. The matrix $[Q]^{(k)}$ is defined in appendix B and is a function of the angle α between the shell principal coordinate x and the material axis 1.

The elastic strain energy U_S of the shell is given by

$$U_S = \frac{1}{2}\sum_{k=1}^{K}\int_0^{2\pi}\int_0^{L}\int_{h^{(k-1)}}^{h^{(k)}} \left(\sigma_x^{(k)}\varepsilon_{xx} + \sigma_\theta^{(k)}\varepsilon_{\theta\theta} + \tau_{x\theta}^{(k)}\gamma_{x\theta} + \tau_{xz}^{(k)}\gamma_{xz} + \tau_{\theta z}^{(k)}\gamma_{\theta z}\right)\left(1 + \frac{z}{R}\right) \mathrm{d}x\, R\, \mathrm{d}\theta\, \mathrm{d}z, \tag{2.9}$$

where K is the total number of layers in the laminated shell and $(h^{(k-1)}, h^{(k)})$ are the z coordinates of the top and bottom surfaces of the kth layer.

The vector of the unknown coefficients is introduced for brevity,

$$\mathbf{q} = \{u_{1,n,c}, u_{2,n,c}, \ldots, u_{1,n,s}, \ldots, v_{1,n,c}, v_{2,n,c}, \ldots, w_{1,n,c}, w_{2,n,c}, \ldots, \phi_{1_{1,n,c}}, \phi_{1_{2,n,c}}, \ldots, \phi_{2_{1,n,c}}, \phi_{2_{2,n,c}}, \ldots\}^{\mathrm{T}}, \tag{2.10}$$

and $n = 0, \ldots, N$. The dimension of $\mathbf{q}$ is $\bar{N}$. The kinetic and potential energies of the shell can be written in vectorial notation

$$T_S = \dot{\mathbf{q}}^{\mathrm{T}}\mathbf{M_S}\dot{\mathbf{q}} \tag{2.11a}$$

and

$$U_S = \mathbf{q}^{\mathrm{T}}\mathbf{K_S}\mathbf{q}, \tag{2.11b}$$

where $\mathbf{M_S}$ and $\mathbf{K_S}$ are the mass and stiffness matrices of the shell, respectively. The natural modes are obtained by solving the following Galerkin equation:

$$-\omega^2\mathbf{M_S}\mathbf{q} + \mathbf{K_S}\mathbf{q} = 0, \tag{2.12}$$

which gives the natural frequencies ω (square root of the eigenvalues) and the natural modes of vibration $\mathbf{q}$ (eigenvectors).

3. Second step: building the reduced-order nonlinear model

A finite number of natural modes, computed by using equation (2.12), are now used to discretize the nonlinear problem. They are defined on the whole structure and allow a reduced-order model to be built with a reasonably small number of degrees of freedom. The small dimension of the reduced-order problem allows continuation technique and bifurcation analysis to be used to obtain the full path of solutions to forced vibration around a resonance. The selection of the natural modes is tricky, and no clear procedure is now available for this operation. In particular, here the selection of the natural modes for the correct simulation of an angle-ply laminated circular cylindrical shell is shown and it is tested versus results obtained by the author with a different discretization technique [25]. This problem is of particular interest because it shows that not only the lowest frequency natural modes have to be retained in the model for accurate simulation, but also axisymmetric terms must be retained for the symmetry of the structure. Moreover, both families of axisymmetric modes with prevalent axial and radial displacements have to be retained. However, for asymmetric modes, only those with prevalent radial displacement have to be retained. Such a non-intuitive conclusion has been reached by developing and integrating many different reduced-order models. They have shown that completely wrong results, not even reported in the present manuscript, are obtained if axisymmetric modes with prevalent axial displacements are neglected.

Assuming harmonic force excitation in the radial direction at the shell mid-length, the model can be built for any resonance of the lowest flexural (i.e. with prevalent radial displacement, which are usually the lowest frequency ones) mode with n circumferential waves by using the following natural modes: (i) the first flexural mode $\mathbf{w}_{1,n,\mathrm{c}}$ with n circumferential waves ($m=1, n$) and its companion $\mathbf{w}_{1,n,\mathrm{s}}$; (ii) the first three flexural modes with $2n$ circumferential waves and their companions, i.e. $\mathbf{w}_{1,2n,\mathrm{c}}$, $\mathbf{w}_{2,2n,\mathrm{s}}$, $\mathbf{w}_{3,2n,\mathrm{c}}$, $\mathbf{w}_{1,2n,\mathrm{s}}$, $\mathbf{w}_{2,2n,\mathrm{c}}$, $\mathbf{w}_{3,2n,\mathrm{s}}$; and (iii) the axisymmetric modes (only those axisymmetric modes that are symmetric with respect to a plane cutting the shell at half length, denoted, for example, by the subscript 1sym for the first symmetric one) with prevalent radial displacement $\mathbf{w}_{(1\mathrm{sym},0)\mathrm{r}}$, $\mathbf{w}_{(2\mathrm{sym},0)\mathrm{r}}$, $\mathbf{w}_{(3\mathrm{sym},0)\mathrm{r}}$, and with prevalent axial displacement $\mathbf{w}_{(1\mathrm{sym},0)\mathrm{a}}$, $\mathbf{w}_{(2\mathrm{sym},0)\mathrm{a}}$, $\mathbf{w}_{(3\mathrm{sym},0)\mathrm{a}}$. Even if the contribution of the axisymmetric generalized coordinates is small with respect to the global vibration amplitudes, they must be retained in the model in order to have an accurate prediction of the shell nonlinearity. If they are neglected, a wrong strong hardening behaviour is predicted. In fact, these generalized coordinates are associated with the dynamic axisymmetric contraction during large-amplitude vibration and must be retained in the expansion in order to avoid large non-physical in-plane stretching of the shell. In fact, thin shells bend easily but they are very stiff to in-plane stretching. Instead, companion modes have to be retained in the expansion owing to the 1 : 1 internal resonance. Here, the following notation has been used for natural modes:

$$\mathbf{w}_{1,n,\mathrm{c}}(x,\theta)=\left(\frac{1}{w^{(1,n,\mathrm{c})}_{1,n,\mathrm{c}}}\right)\left\{u^{(1,n,\mathrm{c})}(x,\theta),v^{(1,n,\mathrm{c})}(x,\theta),w^{(1,n,\mathrm{c})}(x,\theta),\phi_1^{(1,n,\mathrm{c})}(x,\theta),\phi_2^{(1,n,\mathrm{c})}(x,\theta)\right\}^{\mathrm{T}}, \quad (3.1)$$

where

$$u^{(1,n,\mathrm{c})}(x,\theta)=\sum_{m=1}^{M}\left[u^{(1,n,\mathrm{c})}_{m,n,\mathrm{c}}\cos(n\theta)+u^{(1,n,\mathrm{c})}_{m,n,\mathrm{s}}\sin(n\theta)\right]\cos(\lambda_m x), \quad (3.2a)$$

$$v^{(1,n,\mathrm{c})}(x,\theta)=\sum_{m=1}^{M}\left[v^{(1,n,\mathrm{c})}_{m,n,\mathrm{c}}\sin(n\theta)+v^{(1,n,\mathrm{c})}_{m,n,\mathrm{s}}\cos(n\,\theta)\right]\sin(\lambda_m x), \quad (3.2b)$$

$$w^{(1,n,\mathrm{c})}(x,\theta)=\sum_{m=1}^{M}\left[w^{(1,n,\mathrm{c})}_{m,n,\mathrm{c}}\cos(n\theta)+w^{(1,n,\mathrm{c})}_{m,n,\mathrm{s}}\sin(n\theta)\right]\sin(\lambda_m x), \quad (3.2c)$$

$$\phi_1^{(1,n,c)}(x,\theta)=\sum_{m=1}^{M}\left[\phi_{1_{m,n,c}}^{(1,n,c)}\cos(n\theta)+\phi_{1_{m,n,s}}^{(1,n,c)}\sin(n\theta)\right]\cos(\lambda_m x) \tag{3.2d}$$

and

$$\phi_2^{(1,n,c)}(x,\theta)=\sum_{m=1}^{M}\left[\phi_{2_{m,n,c}}^{(1,n,c)}\sin(n\theta)+\phi_{2_{m,n,s}}^{(1,n,c)}\cos(n\theta)\right]\sin(\lambda_m x), \tag{3.2e}$$

where the superscript indicates that the coefficients, introduced in equation (2.3*a–e*), have to be taken for the natural mode indicated in the subscript, i.e. for mode $(1,n,c)$ in this case; the corresponding eigenvector is indicated by $\mathbf{q}^{(1,n,c)}$. In equation (3.1), the mode shape has been normalized with respect to the amplitude $w_{1,n,c}^{(1,n,c)}$ of the dominant flexural component of mode $(1,n,c)$. For mode $\mathbf{w}_{(1\mathrm{sym},0)\mathrm{r}}$, the normalization coefficient is $w_{1\mathrm{sym},0}^{(1\mathrm{sym},0)\mathrm{r}}$ and so on for other natural modes.

The vector $\mathbf{w}$ of the middle plane displacements and rotations of the shell is defined as

$$\mathbf{w}(x,\theta,t)=\{u(x,\theta,t),v(x,\theta,t),w(x,\theta,t),\phi_1(x,\theta,t),\phi_2(x,\theta,t)\}^{\mathrm{T}}, \tag{3.3}$$

and it can be discretized by using the selected natural modes as follows:

$$\begin{aligned}\mathbf{w}(x,\theta,t)=&\,g_1(t)\mathbf{w}_{1,n,c}+g_2(t)\mathbf{w}_{1,n,s}+g_3(t)\mathbf{w}_{(1\mathrm{sym},0)\mathrm{r}}+g_4(t)\mathbf{w}_{(2\mathrm{sym},0)\mathrm{r}}+g_5(t)\mathbf{w}_{(3\mathrm{sym},0)\mathrm{r}}\\&+g_6(t)\mathbf{w}_{(1\mathrm{sym},0)\mathrm{a}}+g_7(t)\mathbf{w}_{(2\mathrm{sym},0)\mathrm{a}}+g_8(t)\mathbf{w}_{(3\mathrm{sym},0)\mathrm{a}}+g_9(t)\mathbf{w}_{1,2n,c}\\&+g_{10}(t)\mathbf{w}_{1,2n,s}+g_{11}(t)\mathbf{w}_{2,2n,c}+g_{12}(t)\mathbf{w}_{2,2n,s}+g_{13}(t)\mathbf{w}_{3,2n,c}+g_{14}(t)\mathbf{w}_{3,2n,s},\end{aligned} \tag{3.4}$$

where $g_i(t)$ are the modal coordinates, which are time functions, expressing the degrees of freedom of the discretized reduced-order system. Equation (3.4) gives the recipe to discretize a circular cylindrical shell with uniform boundary conditions and any lamination sequence, even in the case of moderate geometrical imperfections, which have to be introduced in the first step (linear) of the analysis.

Additional modes can be included in the model (3.4), but they will have a very small contribution, whereas those indicated here are important for good accuracy of the nonlinear response. In the case of internal resonance with modes with a different number of circumferential modes, those also have to be included in the model, but this is a special case that can be verified by observing the integer relationship among the natural frequencies and their combinations in the first linear step of the analysis.

The middle surface of the shell is loaded by distributed forces per unit area q_x, q_θ and q_z acting in the x, θ and z directions, respectively. In this study, only a single harmonic force normal to the shell surface is considered; therefore, $q_x=q_\theta=0$. The external-distributed load q_z applied to the shell, owing to the normal concentrated force $\tilde{f}$, is given by

$$q_z=\tilde{f}\delta(x-\tilde{x})\delta(R\theta-R\tilde{\theta})\cos(\omega t), \tag{3.5}$$

where ω is the excitation frequency, t is the time, δ is the Dirac delta function, $\tilde{f}$ gives the force amplitude positive in the z-direction, and $\tilde{x}$ and $\tilde{\theta}$ give the position of the point of application of the force. Here, the point excitation is located at the centre of shell, that is, $\tilde{x}=L/2$, $\tilde{\theta}=0$. Equation (3.5) is correct assuming that the angle $0\le\theta\le2\pi$; actually, equation (3.5) should work for any angle, because the shell is periodic in θ with period 2π, then equation (3.5) can be replaced with the more complicated expression

$$q_z=\tilde{f}\delta(x-\tilde{x})\sum_{n=0}^{\infty}\delta[R\theta-R(\tilde{\theta}+2\pi n)]\cos(\omega t).$$

This specific dynamic force excites directly the mode $\mathbf{w}_{1,n,c}$, which takes the name of the driven mode. On the other hand, the mode $\mathbf{w}_{1,n,s}$ is not directly excited, because the force is applied at a node for this mode. Therefore, $\mathbf{w}_{1,n,s}$ is named the companion mode, because it is excited only by nonlinear interaction through a 1 : 1 internal resonance between $\mathbf{w}_{1,n,c}$ and $\mathbf{w}_{1,n,s}$. The virtual

work W carried out by the external forces is given by

$$W = \int_0^L \int_0^{2\pi} (q_x u + q_y v + q_z w) \mathrm{d}\, x\, R\, \mathrm{d}\theta = \tilde{f} \cos(\omega t)[w(x,\theta,t)]_{x=L/2,\theta=0}. \tag{3.6}$$

The non-conservative damping forces are assumed to be of viscous type and are taken into account by using the Rayleigh dissipation function

$$F = \frac{1}{2} c \int_0^L \int_0^{2\pi} (\dot{u}^2 + \dot{v}^2 + \dot{w}^2 + h^2 \dot{\phi}_1^2 + h^2 \dot{\phi}_2^2) \mathrm{d}\, x\, R\, \mathrm{d}\theta, \tag{3.7}$$

where c has a different value for each natural mode; in particular

$$F = \frac{1}{2} \frac{L\pi}{2} \left[\sum_{i=1}^{14} c_i \frac{\dot{g}_i(t)^2}{h^2} \right]. \tag{3.8}$$

In equation (3.8), displacements are non-dimensionalized dividing by h, whereas rotations are already non-dimensional. The damping coefficient c_i is related to the modal damping ratio ζ_i that can be experimentally evaluated by $\zeta_i = c_i/(2\mu_i \omega_i)$, where ω_i is the natural circular frequency of mode i and μ_i is the modal mass of the same mode.

The time-dependent vector of the modal coordinates is defined by

$$\mathbf{g} = \{g_1, g_2, \ldots, g_{14}\}^{\mathrm{T}}. \tag{3.9}$$

The generalized forces Q_i are obtained by differentiation of the Rayleigh dissipation function and of the virtual work carried out by external forces,

$$Q_i = -\frac{\partial F}{\partial \dot{g}_i} + \frac{\partial W}{\partial g_i}. \tag{3.10}$$

The Lagrange equations of motion are

$$\frac{\mathrm{d}}{\mathrm{d}t} \left(\frac{\partial T_{\mathrm{S}}}{\partial \dot{g}_i} \right) - \frac{\partial T_{\mathrm{S}}}{\partial g_i} + \frac{\partial U_{\mathrm{S}}}{\partial g_i} = Q_i \quad i = 1, \ldots, 14, \tag{3.11}$$

where $\partial T_{\mathrm{S}}/\partial g_i = 0$. The complicated term, derived from the potential energy of the shell, giving quadratic and cubic nonlinearities, can be written in the form

$$\frac{\partial U_{\mathrm{S}}}{\partial g_i} = \sum_{j=1}^{14} \gamma_{i,j} g_j + \sum_{j,k=1}^{14} \gamma_{i,j,k} g_j g_k + \sum_{j,k,l=1}^{14} \gamma_{i,j,k,l} g_j g_k g_l, \quad i = 1, \ldots, 14, \tag{3.12}$$

where the coefficients γ have long expressions that also include geometrical imperfections. In equation (3.12), there are quadratic and cubic terms.

For shells with rotary inertia, inertial coupling arises in the equations of motion (see equation (2.5)), so that they cannot be immediately transformed in the first-order form required for numerical integration. In particular, the equations of motion take the following form:

$$\mathbf{M}\ddot{\mathbf{g}} + \mathbf{C}\dot{\mathbf{g}} + \{k(\mathbf{g})\} = \mathbf{f_0} \cos(\omega t), \tag{3.13}$$

where $\mathbf{M}$ is the non-diagonal mass matrix of dimension 14×14 (14 being the number of degrees of freedom), $\mathbf{C}$ is the damping matrix, $\mathbf{f}_0$ is the vector of excitation amplitudes, $\mathbf{g}$ is the vector of the modal coordinates, defined in equation (2.6), and

$$\{k(\mathbf{g})\} = \begin{Bmatrix} k_1(\mathbf{g}) \\ \vdots \\ k_{14}(\mathbf{g}) \end{Bmatrix}, \quad \text{with} \quad k_i(\mathbf{g}) = \frac{\partial U_{\mathrm{S}}}{\partial g_i}, \tag{3.14}$$

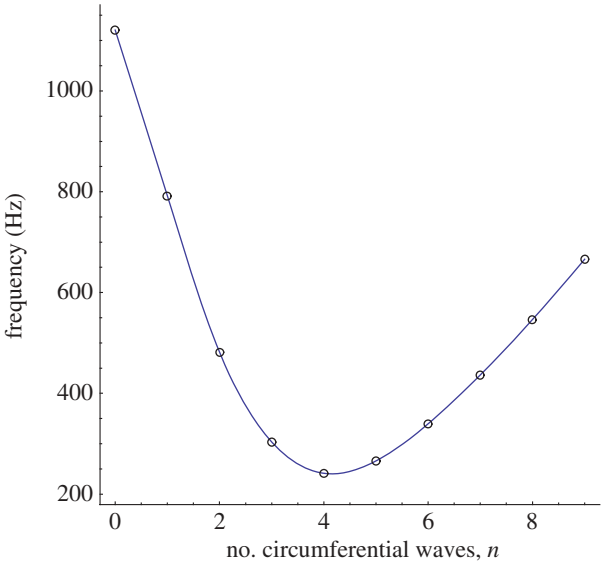

Figure 2. First natural frequency of modes with a different number n of circumferential waves of the $0/30^\circ$ laminated circular cylindrical shell; calculations with model $M = 4$; mode $n = 1$ is torsional. (Online version in colour.)

is the vector containing the stiffness terms (including linear and nonlinear terms) appearing in each one of the 14 equations of motion. Equation (3.13) is pre-multiplied by $\mathbf{M}^{-1}$ in order to diagonalize the mass matrix, as a consequence that the matrix $\mathbf{M}$ is always invertible; the result is

$$\mathbf{I}\ddot{\mathbf{g}} + \mathbf{M}^{-1}\mathbf{C}\dot{\mathbf{g}} + \mathbf{M}^{-1}\{k(\mathbf{g})\} = \mathbf{M}^{-1}\mathbf{f_0}\cos(\omega t). \tag{3.15}$$

Equation (3.15) is in the form suitable for numerical integration.

4. Numerical results

A simply supported, imperfection-free, laminated circular cylindrical shell made of graphite/epoxy layers has been investigated: $R = 0.15\,\mathrm{m}$, $L = 0.52\,\mathrm{m}$, $h = 0.003\,\mathrm{m}$, $E_1 = 50 \times 10^9\,\mathrm{Pa}$, $E_2 = 2 \times 10^9\,\mathrm{Pa}$, $G_{12} = G_{13} = 1 \times 10^9\,\mathrm{Pa}$, $G_{23} = 0.4 \times 10^9\,\mathrm{Pa}$, $\nu_{12} = \nu_{23} = 0.25$ and $\rho = 1500\,\mathrm{kg\,m^{-3}}$. This is a thin shell, being $R/h = 50$. The shell is made of two layers $0/30^\circ$ of the same thickness ($\alpha = 0$ for the internal layer); this choice has been made to have significant skewness in the mode shapes. The linear natural frequencies of the shell are given for modes with $m = 1$ longitudinal half-waves as a function of the number n of circumferential waves in figure 2. The natural frequencies calculated with models with a different number of longitudinal terms M in equations (2.3) are given in table 1; the first mode ($m = 1$) for a different number of circumferential waves n is given. These natural frequencies are for flexural modes (i.e. with prevalent radial displacement w) except for the torsional mode for $n = 1$. The fundamental mode is obtained for $n = 4$ and its natural frequency is 241.4 Hz (with model $M = 4$).

The most important mode shapes used in equation (3.4) to discretize the nonlinear vibration problem for the radial mode with $n = 3$ circumferential waves are presented in figure 3. It is possible to observe in figure 3*a*, which is for mode ($m = 1$, $n = 3$) with prevalent radial displacement, that some twisting of the nodal lines parallel to the longitudinal axis is present; this is due to the angle-ply lamination sequence, as discussed in Amabili [25]. Modes with $n = 6$ circumferential waves are shown in figure 3*b*,*c* because they appear in equation (3.4). Also axisymmetric modes ($n = 0$) are shown in figure 3*d*–*f*, but only those symmetric with respect to the mid-length because they appear in equation (3.4). In figure 3, only modes with prevalent radial displacement are shown.

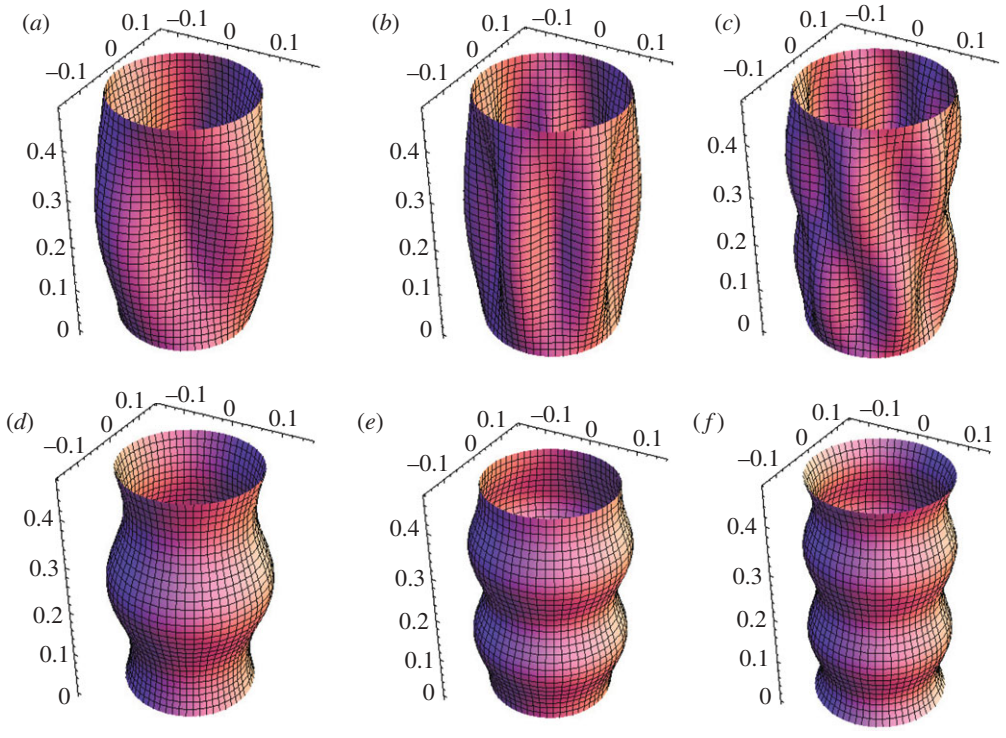

Figure 3. Mode shapes for the radial displacement w of the $0/30^\circ$ laminated circular cylindrical shell; calculations with model $M = 4$. (*a*) $n = 3$, $m = 1$, 303.8 Hz; (*b*) $n = 6$, $m = 1$, 339.6 Hz; (*c*) $n = 6$, $m = 2$, 439.9 Hz; (*d*) $n = 0$, first symmetric mode, 1291.8 Hz; (*e*) $n = 0$, second symmetric mode, 1466.6 Hz; (*f*) $n = 0$, third symmetric mode, 1655.3 Hz. (Online version in colour.)

Table 1. Comparison of the natural frequencies (Hz) obtained with a different number of axial terms M in the expansions for the $0/30^\circ$ laminated shell; modes with a different number n of circumferential waves.

n	$M = 4$	$M = 3$
0	1120.91	1123.73
1	791.55	798.97
2	481.55	485.99
3	303.77	305.81
4	241.44	242.19
5	266.00	266.22
6	339.59	339.63
7	436.71	436.91
8	546.14	546.88
9	665.85	668.85

The nonlinear forced vibration response under harmonic excitation in the spectral neighbourhood of the resonance of mode ($m = 1$, $n = 3$) with prevalent radial displacement is presented in figure 4. For convenience, a non-dimensionalization of the harmonic force excitation acting in the radial direction is introduced. The non-dimensional force f is defined as $f = \tilde{f}/(h\omega_{1n}^2\mu)$, where μ is the modal mass of mode ($m = 1$, $n = 3$) for the radial displacement w, given by $\mu = \rho h R\pi L/2$. A non-dimensional harmonic point force excitation of amplitude $f = 0.00437$

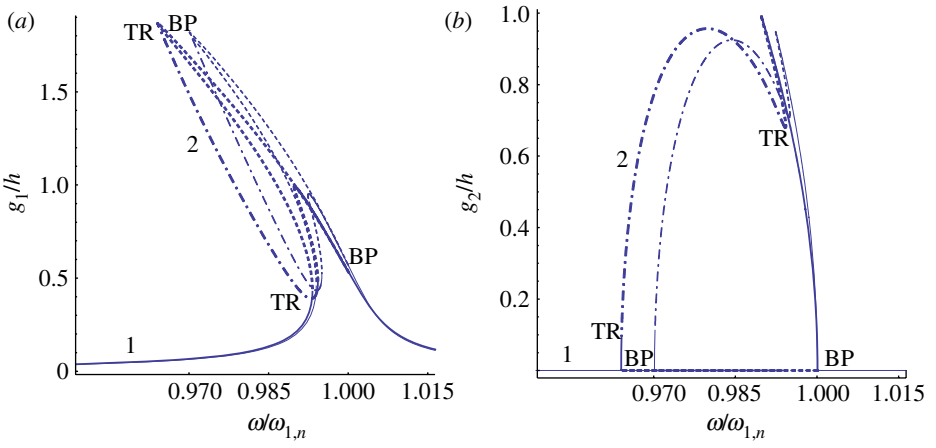

Figure 4. Frequency–response curve of the 0/30° laminated circular cylindrical shell ($n = 3$) obtained with the natural mode reduced-order model (thick lines) versus the results presented in Amabili [25] with model $M = 2$ (37 degrees of freedom) shown in thin lines. Solid line, stable periodic solution; dash dotted line, stable quasi-periodic solution; dashed line, unstable solutions; BP, pitchfork bifurcation; TR, Neimark–Sacker bifurcation; 1, branch 1; 2, branch 2. (*a*) Maximum of the generalized coordinate g_1/h (driven mode); (*b*) maximum of the generalized coordinate g_2/h (companion mode). (Online version in colour.)

and frequency ω applied at shell mid-length is assumed. A modal damping coefficient $\varsigma_{1,n} = 0.001$ has been used for all the generalized coordinates having $n \neq 0$. For the axisymmetric coordinates ($n = 0$), a damping proportionally increasing with frequency has been assumed. The nonlinear equations of motion have been integrated by using the software AUTO [32] for continuation and bifurcation analysis by using the pseudo-arclength continuation method, starting at zero force from the trivial solution. The solution has been initially continued with the excitation amplitude as the parameter and fixed excitation frequency. Once the desired excitation level has been reached, the solution has been continued by using the excitation frequency as the continuation parameter. Pitchfork bifurcations (BPs) and Neimark–Sacker bifurcations are detected in figure 4. Results show the response computed by using the reduced-order model based on natural modes with the 14 degrees of freedom indicated in equation (3.4), compared with results obtained in Amabili [25] with 37 degrees of freedom with an ad hoc constructed reduced-order model. As will be shown later, the present results are more accurate because they take into account a larger number of axial terms ($M = 4$), but at the same time they are obtained with a smaller model saving computational time.

The branch 1 of the nonlinear response in figure 4 corresponds to vibration with zero amplitude of the companion mode $g_2(t)$. Branch 1 has two BPs at $\omega/\omega_{1,n} = 0.964$ and at 1.0001, where branch 2 appears. This new branch corresponds to participation of both $g_1(t)$ and $g_2(t)$, giving a travelling-wave response, i.e. nodal lines travel around the shell during vibrations. The companion mode presents a node at the location of the excitation force, and therefore it is not directly excited; its amplitude is different from zero only for large-amplitude vibrations, owing to nonlinear coupling through 1 : 1 internal resonance. In the frequency region where both $g_1(t)$ and $g_2(t)$ are different from zero, they give rise to a travelling wave around the shell; phase shift between the two coordinates is practically equal to $\pi/2$ when the two generalized coordinates have almost the same amplitude, as can be observed comparing figure 4*a*,*b*. This branch appears for sufficiently large excitation. Branch 2 undergoes two Neimark–Sacker (torus) bifurcations, at $\omega/\omega_{1,n} = 0.9641$ and 0.9941. The amplitude-modulated (quasi-periodic) response is indicated in figure 4 on branch 2 for $0.9641 < \omega/\omega_{1,n} < 0.9941$, that is, bracketed by the two Neimark–Sacker bifurcations.

Another comparison of the present reduced-order model versus two larger models presented in Amabili [25] is shown in figure 5 for the generalized coordinate $g_1(t)$ only. As anticipated, figure 5 shows that the present results are more accurate than those in Amabili [25] for $M = 2$

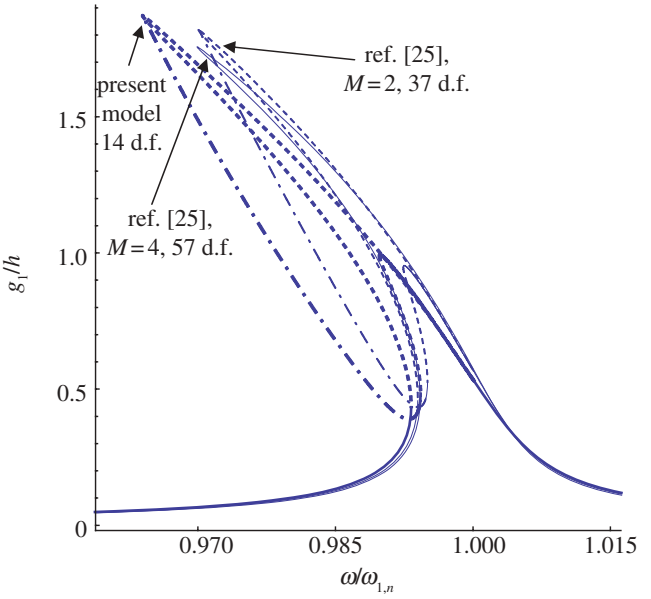

Figure 5. Frequency–response curve of the $0/30^\circ$ laminated circular cylindrical shell obtained by using the present model (natural mode reduced-order model, thick lines) versus the results presented in Amabili [25] with models $M = 2$ and $M = 4$ shown in thin lines; $n = 3$. Solid line, stable periodic solution; dash dotted line, stable quasi-periodic solution; dashed line, unstable solutions. (Online version in colour.)

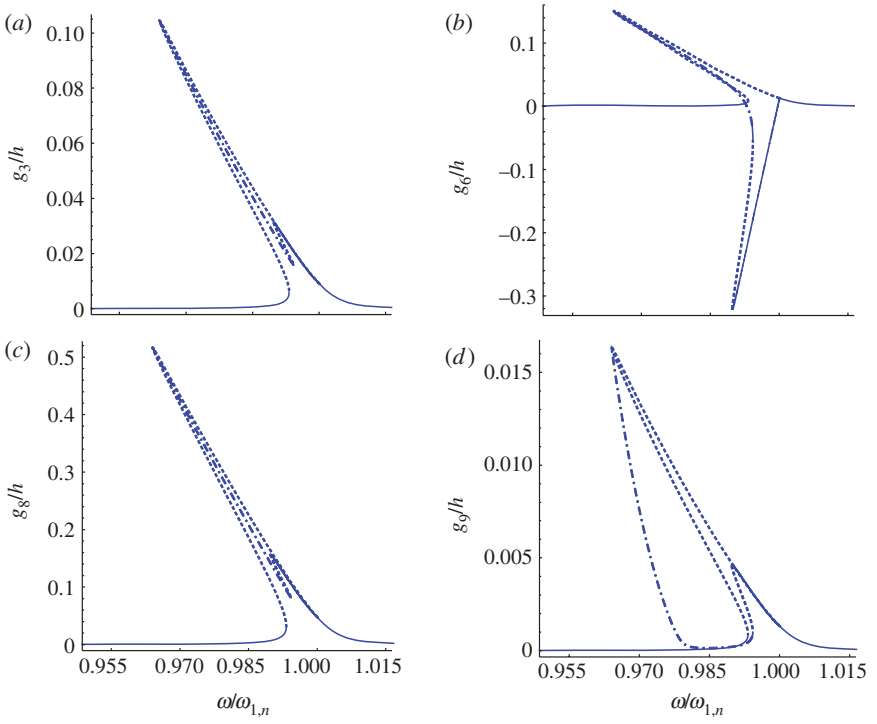

Figure 6. Frequency–response curve of the $0/30^\circ$ laminated circular cylindrical shell ($n = 3$) obtained with the natural mode reduced-order model. Solid line, stable periodic solution; dash dotted line, stable quasi-periodic solution; dashed line, unstable solutions. (*a*) Maximum of the generalized coordinate g_3/h; (*b*) maximum of the generalized coordinate g_6/h; (*c*) maximum of the generalized coordinate g_8/h; (*d*) maximum of the generalized coordinate g_9/h. (Online version in colour.)

and they seem to be better than those with $M=4$ in Amabili [25] because more terms with $2n$ circumferential waves have been considered in the present reduced-order model. An important reduction in the number of degrees of freedom is obtained, even with respect to the ad hoc reduced-order model presented in Amabili [25].

The additional generalized coordinates used in the present model and showing a significant amplitude are given in figure 6*a–d*. Out of those, $g_8(t)$ is the one with the largest displacement and is associated with the third axisymmetric mode (symmetric with respect to the shell mid-length) with prevalent axial displacement. For axisymmetric modes with prevalent radial displacement, $g_3(t)$ is the coordinate with the largest amplitude. In comparison, the contribution of modes with six circumferential waves is small, as indicated by the coordinate $g_9(t)$.

5. Conclusion

A reduced-order model for nonlinear vibrations of angle-ply laminated circular cylindrical shells has been developed by using natural modes of vibration. A recipe for the selection of the modes to be retained in the discretization process is given, which is valid for circular shells with uniform boundary conditions and generic lamination sequence even in the case of moderate geometrical imperfections. The model presents very good results compared with an ad hoc reduced model developed to study the same problem, but it gives a further reduction in the number of degrees of freedom. Reduced-order models based on natural modes of vibration do not have the limitation of losing accuracy increasing the vibration amplitude, as is the case in asymptotic nonlinear normal modes. The method gives models of small size that can be studied by using bifurcation analysis and continuation methods. It seems to have a huge potential to be applied in conjunction with commercial finite-element codes for linear analysis.

M.A. acknowledges the financial support of the NSERC Discovery Grant, Canada Research Chair and Canada Foundation for Innovation (Leader Opportunity Fund) programmes of Canada and the PSR-SIIRI programme of Québec.

Appendix A. The Amabili–Reddy nonlinear higher-order shear deformation theory

The displacements (u_x, u_θ, u_z) of a generic point of the shell at distance z from the middle surface are related to the middle surface displacements by [31]

$$u_x = u + z\phi_1 + z^2\psi_1 + z^3\gamma_1 + z^4\theta_1, \tag{A 1a}$$

$$u_\theta = (1 + z/R)v + z\phi_2 + z^2\psi_2 + z^3\gamma_2 + z^4\theta_2 \tag{A 1b}$$

and

$$u_z = w + z\chi + w_0, \tag{A 1c}$$

where ϕ_1 and ϕ_2 are the rotations of the transverse normals at $z=0$ about the y (y is the curvilinear coordinate $(R+z)\theta$, which is orthogonal to x and z) and x axes, respectively, and ψ_1, ψ_2, γ_1, γ_2, θ_1, θ_2 and χ are functions to be determined in terms of u, v, w, ϕ_1 and ϕ_2, the five variables describing the shell deformation.

Calculations give

$$\psi_1 = -\frac{1}{2}\frac{\partial \chi}{\partial x}, \tag{A 2a}$$

$$\gamma_1 = \frac{-4}{3h^2}\left(\phi_1 + \frac{\partial w}{\partial x}\right), \tag{A 2b}$$

$$\theta_1 = 0, \tag{A 2c}$$

$$\psi_2 = \frac{1}{2R}\phi_2 + \frac{1}{2}\frac{\partial w}{R\partial\theta} - \frac{1}{2}\frac{\partial \chi}{R\partial\theta}, \tag{A 3a}$$

$$\gamma_2 = \frac{-4}{3h^2}\left[\phi_2 + \frac{\partial w}{R\partial\theta} + \frac{h^2}{8R^2}\left(\phi_2 - \frac{\partial w}{R\partial\theta} - R\frac{\partial \chi}{R\partial\theta}\right)\right], \tag{A 3b}$$

$$\theta_2 = \frac{1}{4R}\gamma_2 - \frac{1}{4R^2}\psi_2, \tag{A 3c}$$

$$\chi \simeq 0. \tag{A 4}$$

Equations (A 1*a–c*) are linear in the five variables describing the shell deformation u, v, w, ϕ_1 and ϕ_2.

The strain–displacement equations for the higher-order shear deformation theory, keeping terms up to z^3, are

$$\varepsilon_{xx} = \varepsilon_{x,0} + z\left(k_x^{(0)} + zk_x^{(1)} + z^2k_x^{(2)}\right), \tag{A 5a}$$

$$\varepsilon_{\theta\theta} = \varepsilon_{\theta,0} + z\left(k_\theta^{(0)} + zk_\theta^{(1)} + z^2k_\theta^{(2)}\right), \tag{A 5b}$$

$$\gamma_{x\theta} = \gamma_{x\theta,0} + z\left(k_{x\theta}^{(0)} + zk_{x\theta}^{(1)} + z^2k_{x\theta}^{(2)}\right), \tag{A 5c}$$

$$\gamma_{xz} = \gamma_{xz,0} + z\left(k_{xz}^{(0)} + z\,k_{xz}^{(1)} + z^2k_{xz}^{(2)}\right) \tag{A 5d}$$

and

$$\gamma_{\theta z} = \gamma_{\theta z,0} + z\left(k_{\theta z}^{(0)} + zk_{\theta z}^{(1)} + z^2k_{\theta z}^{(2)}\right), \tag{A 5e}$$

where

$$\varepsilon_{x,0} = \frac{\partial u}{\partial x} + \frac{1}{2}\left[\left(\frac{\partial u}{\partial x}\right)^2 + \left(\frac{\partial v}{\partial x}\right)^2 + \left(\frac{\partial w}{\partial x}\right)^2\right] + \frac{\partial w_0}{\partial x}\frac{\partial w}{\partial x}, \tag{A 6a}$$

$$\varepsilon_{\theta,0} = \frac{1}{R}\frac{\partial v}{\partial\theta} + \frac{w}{R} + \frac{1}{2}\left[\left(\frac{1}{R}\frac{\partial u}{\partial\theta}\right)^2 + \left(\frac{1}{R}\frac{\partial v}{\partial\theta} + \frac{w}{R}\right)^2 + \left(\frac{1}{R}\frac{\partial w}{\partial\theta} - \frac{v}{R}\right)^2\right] + \frac{w_0}{R}\left(\frac{1}{R}\frac{\partial v}{\partial\theta} + \frac{w}{R}\right) + \frac{1}{R}\frac{\partial w_0}{\partial\theta}\left(\frac{1}{R}\frac{\partial w}{\partial\theta} - \frac{v}{R}\right), \tag{A 6b}$$

$$\gamma_{x\theta,0} = \frac{\partial v}{\partial x} + \frac{1}{R}\frac{\partial u}{\partial\theta} + \frac{1}{R}\frac{\partial u}{\partial x}\frac{\partial u}{\partial\theta} + \left(\frac{1}{R}\frac{\partial v}{\partial\theta} + \frac{w}{R}\right)\frac{\partial v}{\partial x} + \frac{\partial w}{\partial x}\left(\frac{1}{R}\frac{\partial w}{\partial\theta} - \frac{v}{R}\right) + \frac{w_0}{R}\frac{\partial v}{\partial x} + \frac{\partial w_0}{\partial x}\left(\frac{1}{R}\frac{\partial w}{\partial\theta} - \frac{v}{R}\right) + \frac{1}{R}\frac{\partial w_0}{\partial\theta}\frac{\partial w}{\partial x}, \tag{A 6c}$$

$$\gamma_{xz,0} = \phi_1 + \frac{\partial w}{\partial x}, \tag{A 6d}$$

$$\gamma_{\theta z,0} = \phi_2 + \frac{1}{R}\frac{\partial w}{\partial\theta} \tag{A 6e}$$

and

$$k_x^{(0)} = \frac{\partial\phi_1}{\partial x}, \tag{A 7a}$$

$$k_x^{(1)} = 0, \tag{A 7b}$$

$$k_x^{(2)} = -\frac{4}{3h^2}\left(\frac{\partial\phi_1}{\partial x} + \frac{\partial^2 w}{\partial x^2}\right), \tag{A 7c}$$

$$k_\theta^{(0)} = \frac{1}{R}\frac{\partial\phi_2}{\partial\theta} - \frac{w}{R^2}, \tag{A 7d}$$

$$k_{\theta}^{(1)} = -\frac{1}{R^2}\left(\frac{1}{2}\frac{\partial \phi_2}{\partial \theta} + \frac{1}{R}\frac{\partial v}{\partial \theta} - \frac{1}{2R}\frac{\partial^2 w}{\partial \theta^2}\right), \tag{A 7e}$$

$$k_{\theta}^{(2)} = -\frac{4}{3h^2}\left(\frac{1}{R}\frac{\partial \phi_2}{\partial \theta} + \frac{1}{R^2}\frac{\partial^2 w}{\partial \theta^2}\right) - \frac{1}{3R^2}\left(\frac{2}{R}\frac{\partial \phi_2}{\partial \theta} + \frac{1}{R^2}\frac{\partial^2 w}{\partial \theta^2}\right), \tag{A 7f}$$

$$k_{x\theta}^{(0)} = \frac{1}{R}\frac{\partial \phi_1}{\partial \theta} + \frac{\partial \phi_2}{\partial x} + \frac{1}{R}\left(\frac{\partial v}{\partial x} - \frac{1}{R}\frac{\partial u}{\partial \theta}\right), \tag{A 7g}$$

$$k_{x\theta}^{(1)} = \frac{1}{R}\left(-\frac{1}{R}\frac{\partial \phi_1}{\partial \theta} + \frac{1}{2}\frac{\partial \phi_2}{\partial x} + \frac{1}{2R}\frac{\partial^2 w}{\partial x \partial \theta}\right), \tag{A 7h}$$

$$k_{x\theta}^{(2)} = -\frac{4}{3h^2}\left(\frac{1}{R}\frac{\partial \phi_1}{\partial \theta} + \frac{\partial \phi_2}{\partial x} + \frac{2}{R}\frac{\partial^2 w}{\partial x \partial \theta}\right) + \frac{1}{6R^2}\left(-\frac{\partial \phi_2}{\partial x} + \frac{1}{R}\frac{\partial^2 w}{\partial x \partial \theta}\right) \tag{A 7i}$$

and

$$k_{xz}^{(0)} = 0, \tag{A 8a}$$

$$k_{xz}^{(1)} = -\frac{4}{h^2}\left(\phi_1 + \frac{\partial w}{\partial x}\right), \tag{A 8b}$$

$$k_{xz}^{(2)} = 0, \tag{A 8c}$$

$$k_{\theta z}^{(0)} = 0, \tag{A 8d}$$

$$k_{\theta z}^{(1)} = -\frac{4}{h^2}\left(\phi_2 + \frac{1}{R}\frac{\partial w}{\partial \theta}\right) + \frac{v}{R^3} \tag{A 8e}$$

and

$$k_{\theta z}^{(2)} = 0. \tag{A 8f}$$

Equations (A 5*d*,*e*) show that the strain and stress distribution through the thickness is parabolic and therefore the shear correction factor is no longer required. Equations (A 6*a*–*c*), giving the middle surface strains, are coincident with those obtained by using Novozhilov nonlinear shell theory [26], which neglects shear deformation and rotary inertia.

Appendix B. From material to shell reference system

Usually, the lamina material axes (1,2) do not coincide with the shell reference axes (x, θ), whereas the 3 axis is coincident with z. Then, the strains and stresses on material axes can be related to the reference axes by using the following invertible expressions:

$$\begin{Bmatrix} \sigma_1 \\ \sigma_2 \\ \tau_{23} \\ \tau_{13} \\ \tau_{12} \end{Bmatrix} = \mathbf{T}_1 \begin{Bmatrix} \sigma_x \\ \sigma_\theta \\ \tau_{\theta z} \\ \tau_{xz} \\ \tau_{x\theta} \end{Bmatrix}, \tag{B 1a}$$

$$\begin{Bmatrix} \varepsilon_{11} \\ \varepsilon_{22} \\ \gamma_{23} \\ \gamma_{13} \\ \gamma_{12} \end{Bmatrix} = \mathbf{T}_2 \begin{Bmatrix} \varepsilon_{xx} \\ \varepsilon_{\theta\theta} \\ \gamma_{\theta z} \\ \gamma_{xz} \\ \gamma_{x\theta} \end{Bmatrix}, \tag{B 1b}$$

where

$$\mathbf{T}_1 = \begin{bmatrix} \cos^2\alpha & \sin^2\alpha & 0 & 0 & 2\sin\alpha\cos\alpha \\ \sin^2\alpha & \cos^2\alpha & 0 & 0 & -2\sin\alpha\cos\alpha \\ 0 & 0 & \cos\alpha & -\sin\alpha & 0 \\ 0 & 0 & \sin\alpha & \cos\alpha & 0 \\ -\sin\alpha\cos\alpha & \sin\alpha\cos\alpha & 0 & 0 & \cos^2\alpha - \sin^2\alpha \end{bmatrix} \tag{B 2}$$

and

$$\mathbf{T}_2 = \begin{bmatrix} \cos^2\alpha & \sin^2\alpha & 0 & 0 & \sin\alpha\cos\alpha \\ \sin^2\alpha & \cos^2\alpha & 0 & 0 & -\sin\alpha\cos\alpha \\ 0 & 0 & \cos\alpha & -\sin\alpha & 0 \\ 0 & 0 & \sin\alpha & \cos\alpha & 0 \\ -2\sin\alpha\cos\alpha & 2\sin\alpha\cos\alpha & 0 & 0 & \cos^2\alpha - \sin^2\alpha \end{bmatrix}, \tag{B 3}$$

α being the angle between the shell principal coordinate x and the material axis 1.

It can be shown that

$$(\mathbf{T}_1^{-1})^{\mathrm{T}} = \mathbf{T}_2. \tag{B 4}$$

Therefore, it is convenient to introduce the matrix $[Q]^{(k)}$ given by

$$[Q]^{(k)} = [\mathbf{T}_2^{\mathrm{T}}\mathbf{C}\mathbf{T}_2]^{(k)}, \tag{B 5}$$

where $\mathbf{C}$ is the 5×5 matrix of c_{ij} and G_{ij} coefficients in equation (2.6). As a consequence of the discontinuous variation of the stiffness matrix $[Q]^{(k)}$ from layer to layer, the stresses may be discontinuous from layer to layer.

References

1. Carr J. 1981 *Applications of centre manifold theory*. New York, NY: Springer.
2. Guckenheimer J, Holmes P. 1983 *Non-linear oscillations, dynamical systems and bifurcations of vector field*. New York, NY: Springer.
3. Iooss G, Adelmeyer M. 1998 *Topics in bifurcation theory*, 2nd edn. New York, NY: World Scientific.
4. Rosenberg RM. 1966 On non-linear vibrations of systems with many degrees of freedom. *Adv. Appl. Mech.* **9**, 155–242. (doi:10.1016/S0065-2156(08)70008-5)
5. Mikhlin YV. 1995 Matching of local expansions in the theory of non-linear vibrations. *J. Sound Vib.* **182**, 577–588. (doi:10.1006/jsvi.1995.0218)
6. Vakakis AF, Manevich LI, Mikhlin YV, Pilipchuk VN, Zevin AA. 1996 *Normal modes and localization in non-linear systems*. New York, NY: Wiley.
7. Shaw S, Pierre C. 1991 Non-linear normal modes and invariant manifolds. *J. Sound Vib.* **150**, 170–173. (doi:10.1016/0022-460X(91)90412-D)
8. Jézéquel L, Lamarque CH. 1991 Analysis of non-linear dynamical systems by the normal form theory. *J. Sound Vib.* **149**, 429–459. (doi:10.1016/0022-460X(91)90446-Q)
9. Touzé C, Amabili M. 2006 Non-linear normal modes for damped geometrically non-linear systems: application to reduced-order modeling of harmonically forced structures. *J. Sound Vib.* **298**, 958–981. (doi:10.1016/j.jsv.2006.06.032)
10. Dowell EH. 1982 Flutter of a buckled plate as an example of chaotic motion of a deterministic autonomous system. *J. Sound Vib.* **85**, 333–344. (doi:10.1016/0022-460X(82)90259-0)
11. Gonçalves PB, Batista RC. 1988 Non-linear vibration analysis of fluid-filled cylindrical shells. *J. Sound Vib.* **127**, 133–143. (doi:10.1016/0022-460X(88)90354-9)
12. Popov AA, Thompson JMT, McRobie FA. 1998 Low dimensional models of shell vibrations. Parametrically excited vibrations of cylindrical shells. *J. Sound Vib.* **209**, 163–186. (doi:10.1006/jsvi.1997.1279)
13. Amabili M. 2003 Comparison of shell theories for large-amplitude vibrations of circular cylindrical shells: Lagrangian approach. *J. Sound Vib.* **264**, 1091–1125. (doi:10.1016/S0022-460X(02)01385-8)
14. Zahorian SA, Rothenberg M. 1981 Principal component analysis for low-redundancy encoding of speech spectra. *J. Acoust. Soc. Am.* **69**, 519–524. (doi:10.1121/1.385539)
15. Aubry N, Holmes P, Lumley JL, Stone E. 1988 The dynamics of coherent structures in the wall region of a turbulent boundary layer. *J. Fluid. Mech.* **192**, 115–173. (doi:10.1017/S0022112088001818)
16. Sirovich L. 1987 Turbulence and dynamics of coherent structures. I. Coherent structures. *Q. Appl. Math.* **45**, 561–571.
17. Amabili M, Sarkar A, Païdoussis MP. 2003 Reduced-order models for nonlinear vibrations of cylindrical shells via the proper orthogonal decomposition method. *J. Fluids Struct.* **18**, 227–250. (doi:10.1016/j.jfluidstructs.2003.06.002)

18. Kerschen G, Golinval J-C, Vakakis AF, Bergman LA. 2005 The method of proper orthogonal decomposition for dynamical characterization and order reduction of mechanical systems: an overview. *Nonlinear Dyn.* **41**, 147–169. (doi:10.1007/s11071-005-2803-2)
19. McEwan MI, Wright JR, Cooper JE, Leung AYT. 2001 A combined modal/finite element analysis technique for the dynamic response of a non-linear beam to harmonic excitation. *J. Sound Vib.* **243**, 601–624. (doi:10.1006/jsvi.2000.3434)
20. Muravyov AA, Rizzi SA. 2004 Determination of nonlinear stiffness with application to random vibration of geometrically nonlinear structures. *Comp. Struct.* **81**, 1513–1523. (doi:10.1016/S0045-7949(03)00145-7)
21. Mignolet MP, Soize C. 2008 Stochastic reduced order models for uncertain geometrically nonlinear dynamical systems. *Comp. Methods Appl. Mech. Eng.* **197**, 3951–3963. (doi:10.1016/j.cma.2008.03.032)
22. Kurylov Y, Amabili M. 2011 Nonlinear vibrations of clamped-free circular cylindrical shells. *J. Sound Vib.* **330**, 5363–5381. (doi:10.1016/j.jsv.2011.05.037)
23. Lazarus A, Thomas O, Deü J-F. 2012 Finite element reduced order models for nonlinear vibrations of piezoelectric layered beams with application to NEMS. *Finite Elements Anal. Des.* **49**, 35–51. (doi:10.1016/j.finel.2011.08.019)
24. Amabili M, Touzé C. 2007 Reduced-order models for nonlinear vibrations of fluid-filled circular cylindrical shells: comparison of POD and asymptotic nonlinear normal modes methods. *J. Fluids Struct.* **23**, 885–903. (doi:10.1016/j.jfluidstructs.2006.12.004)
25. Amabili M. 2012 Nonlinear vibrations of angle-ply laminated circular cylindrical shells: skewed modes. *Compos. Struct.* **94**, 3697–3709. (doi:10.1016/j.compstruct.2012.05.019)
26. Amabili M. 2008 *Nonlinear vibrations and stability of shells and plates*. New York, NY: Cambridge University Press.
27. Ganapathi M, Varadan TK. 1995 Nonlinear free flexural vibrations of laminated circular cylindrical shells. *Compos. Struct.* **30**, 33–49. (doi:10.1016/0263-8223(94)00025-5)
28. Jansen EL. 2008 The effect of static loading and imperfections on the nonlinear vibrations of laminated cylindrical shells. *J. Sound Vib.* **315**, 1035–1046. (doi:10.1016/j.jsv.2008.02.004)
29. Ribeiro P. 2009 On the influence of membrane inertia and shear deformation on the geometrically non-linear vibrations of open, cylindrical, laminated clamped shells. *Compos. Sci. Technol.* **69**, 176–185. (doi:10.1016/j.compscitech.2008.09.038)
30. Amabili M. 2011 Nonlinear vibrations of laminated circular cylindrical shells: comparison of different shell theories. *Compos. Struct.* **94**, 207–220. (doi:10.1016/j.compstruct.2011.07.001)
31. Amabili M, Reddy JN. 2010 A new non-linear higher-order shear deformation theory for large-amplitude vibrations of laminated doubly curved shells. *Int. J. Non-linear Mech.* **45**, 409–418. (doi:10.1016/j.ijnonlinmec.2009.12.013)
32. Doedel EJ, Champneys AR, Fairgrieve TF, Kuznetsov YA, Sandstede B, Wang X. 1998 *AUTO 97: continuation and bifurcation software for ordinary differential equations* (*with HomCont*). Montreal, Canada: Concordia University.